Hadron Phenomenology in Light-Front Dynamics

Chueng Ji (NCSU) LANL 2002, Aug. 9.

In many physical processes involving hadrons, LFD plays an important role.

e.g. Form Factors : $\ell p \to \ell' p'$

$$\langle p'\lambda' | J^+(0) | p\lambda \rangle = \sum_n$$

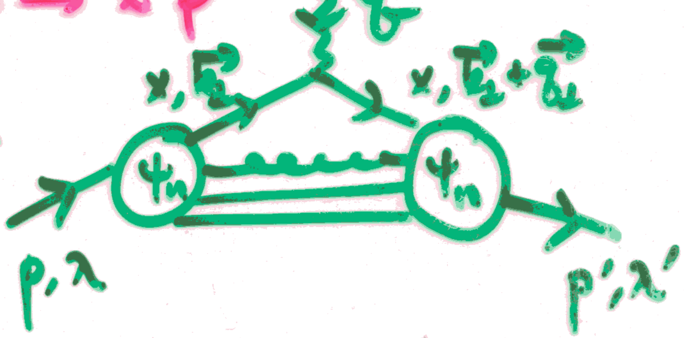

DVCS : $\gamma^* p \to \gamma' p'$

$\langle p'\lambda' | J^\mu(z) J^\nu(0) | p\lambda \rangle$ at large $Q^2 = -q^2$

$$= \sum_n$$

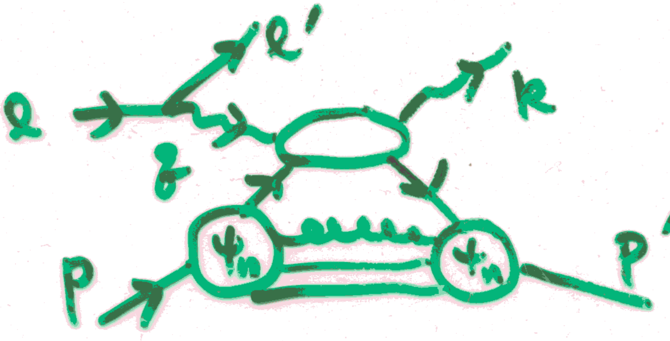

+

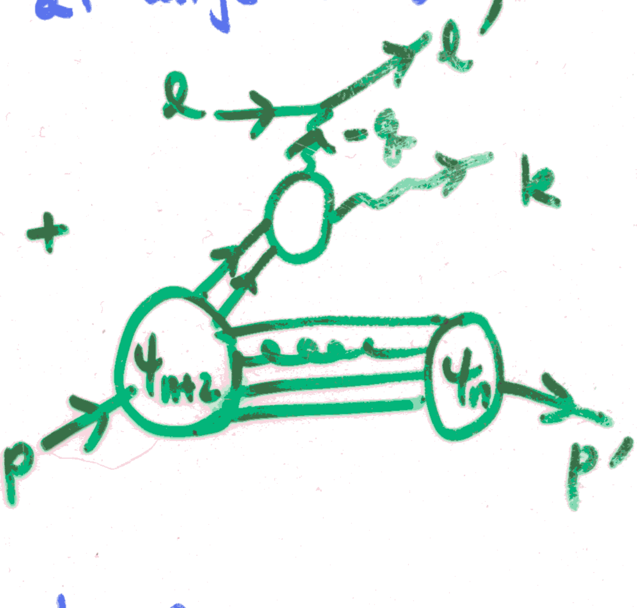

⋮

However, there are also caveats from zero-modes in LFD.

e.g. Helicity $0 \to 0$ Amp for J^+ current, Spin $0 \to 1$ Trans. f.f. ....

Outline

1. Few Caveats in LFD.
   - Zero-modes in J^+ current
   - Treacherous common belief
2. LFCQM Phenomenology
   - Meson spectroscopy
   - Timelike processes
3. GPD Application
   - Continuity at crossover
   - SSA comment
4. Conclusions and Discussions

B. Bakker, H. Choi, C. Ji, PRD65, 116001 (02)
PRD63, 074014 (01)

B. Bakker, C. Ji, PRD65, 073002 (02), PRD62, 074014 (00)

H. Choi, C. Ji, L. Kisslinger, PRD65, 074032 (02), PRD64, 093006 (01)
hep-ph 0204321

H. Choi, C. Ji, PLB513, 330 (01), NPA679, 735 (01), PLB460, 461 (99)
PRD59, 074015 (99), PRD59, 034001 (99), PRD58, 071901 (98 ....

LFD in Exclusive Processes

$q^+ = q^0 + q^3$

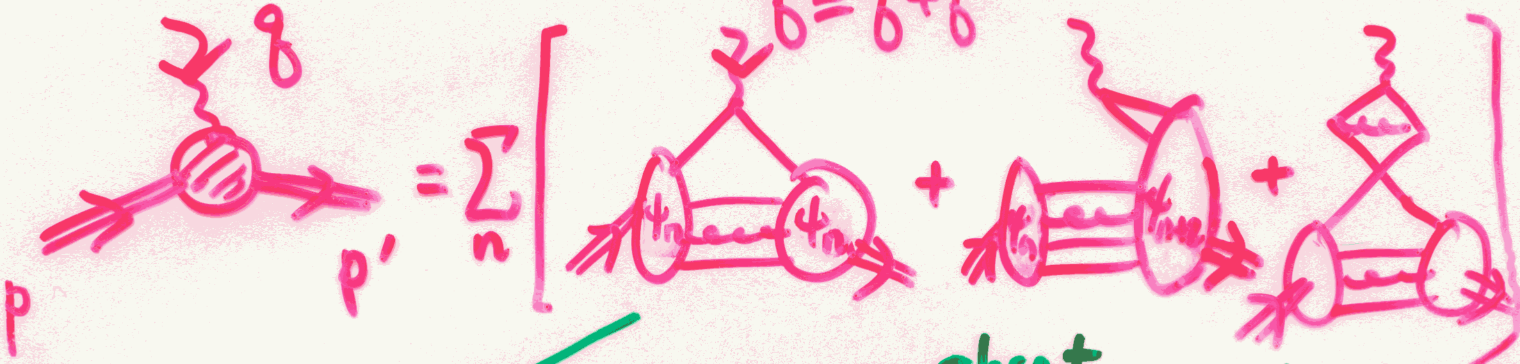

absent if $q^+ = 0$ and J^+

absent due to $p^+ = \frac{p_\perp^2 + m^2}{p^-}$

pQCD factorization for $|q^2| \gg \Lambda_{QCD}^2$

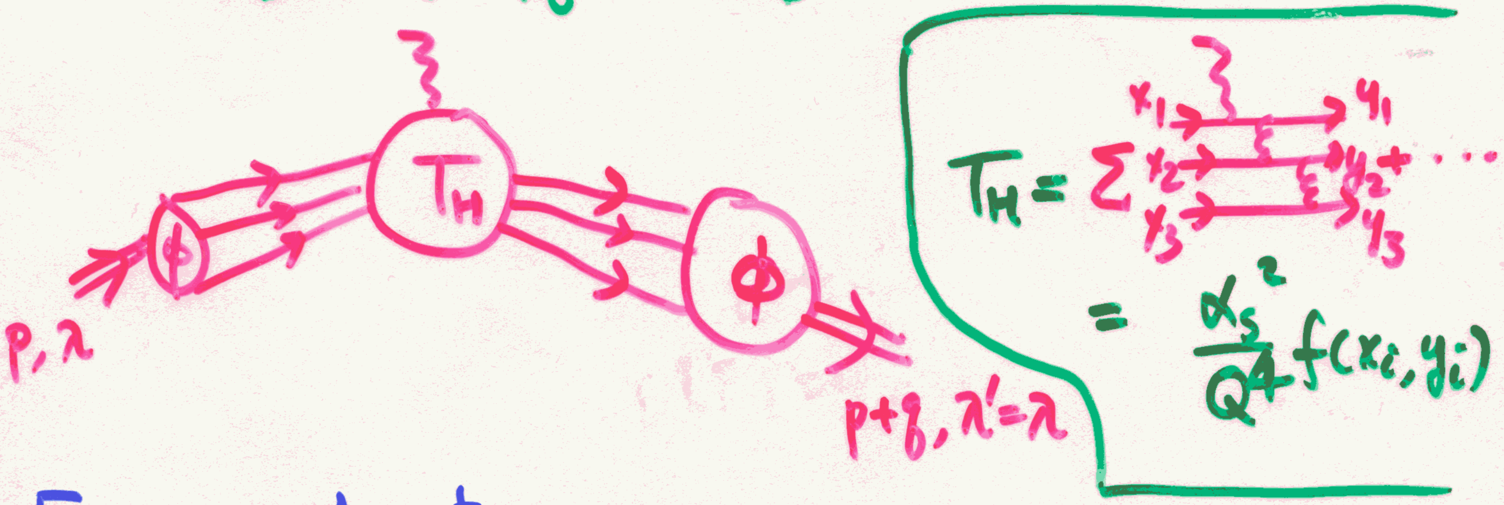

For spin-1 system, PQCD prediction is based on helicity $0 \to 0$ amplitude.

Zero-mode danger in Spin-1 systems:

Deuteron, ρ-meson, $W^\pm$ ...

J. de Melo et al., NPA 631, 574 (98); NPA 650, 219 (99)

Bakker, Choi, Ji, PRD 65, 116001 (02).

Exactly Solvable Model

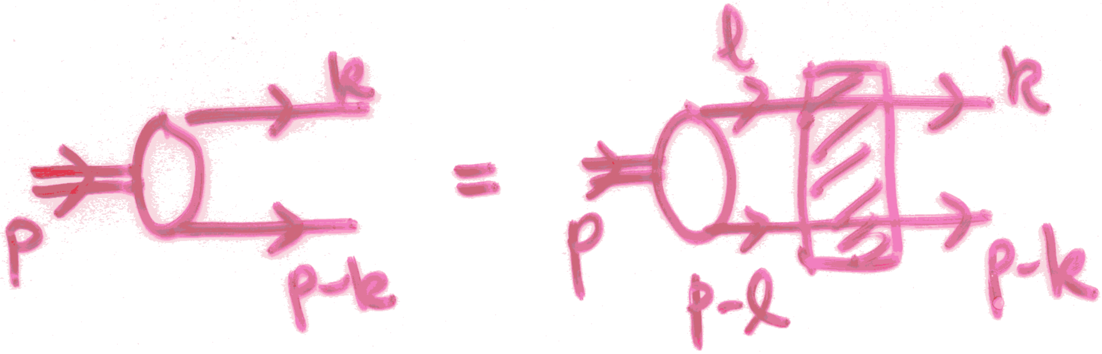

$$(k^2-m^2+i\epsilon)\{(p-k)^2-m^2+i\epsilon\}\,\psi_p(k)$$
$$=\int d^4l\,K(k,l)\,\psi_p(l).$$

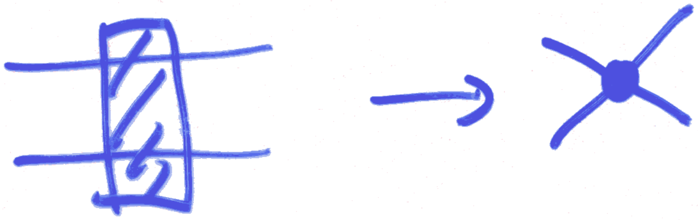

Glazek & Sawicki, Phys. Rev. D41, 2563(90)

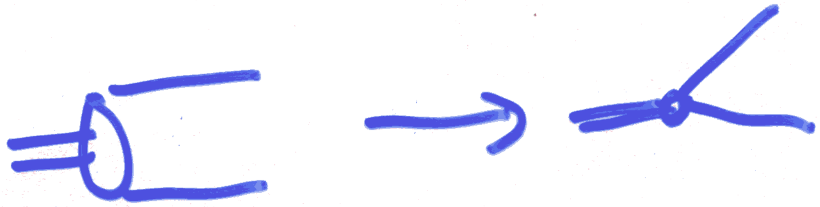

$$\mathcal{L}_{int}=\begin{cases} g\phi\bar{\psi}i\gamma_5\psi \\ g\phi\bar{\psi}\psi \\ g\phi\chi\chi. \end{cases}$$

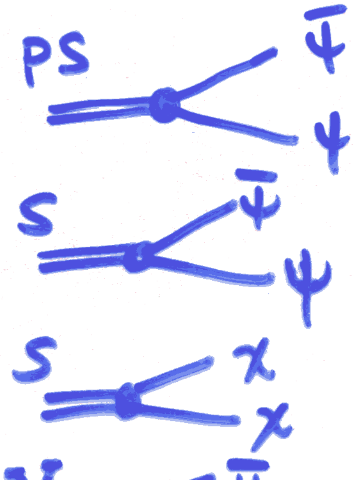

Zero-Mode.

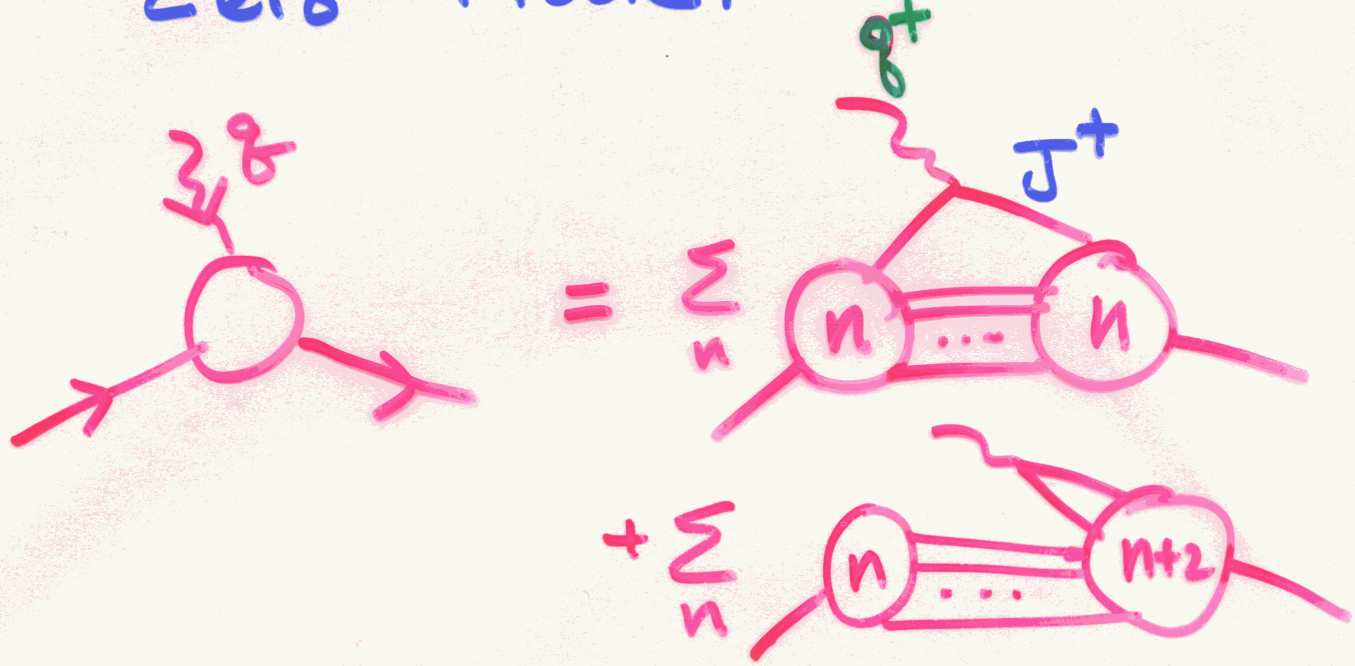

Even if $q^+ \to 0$, the off-diagonal elements do not go away in some cases.

$$\lim_{q^+ \to 0} \int_{p^+}^{p^+ + q^+} dk^+ \left(\cdots \right) \neq 0$$

$$\epsilon(+) = \left(0, \frac{p^r}{p^+}, -\frac{1}{\sqrt{2}}, -\frac{i}{\sqrt{2}}\right)$$

$$\epsilon(0) = \left(\frac{p^+}{m}, \frac{\vec{p}_\perp^{\,2} - m^2}{2mp^+}, \frac{p^1}{m}, \frac{p^2}{m}\right)$$

$$\epsilon(-) = \left(0, \frac{p^l}{p^+}, \frac{1}{\sqrt{2}}, -\frac{i}{\sqrt{2}}\right).$$

Model Calculation

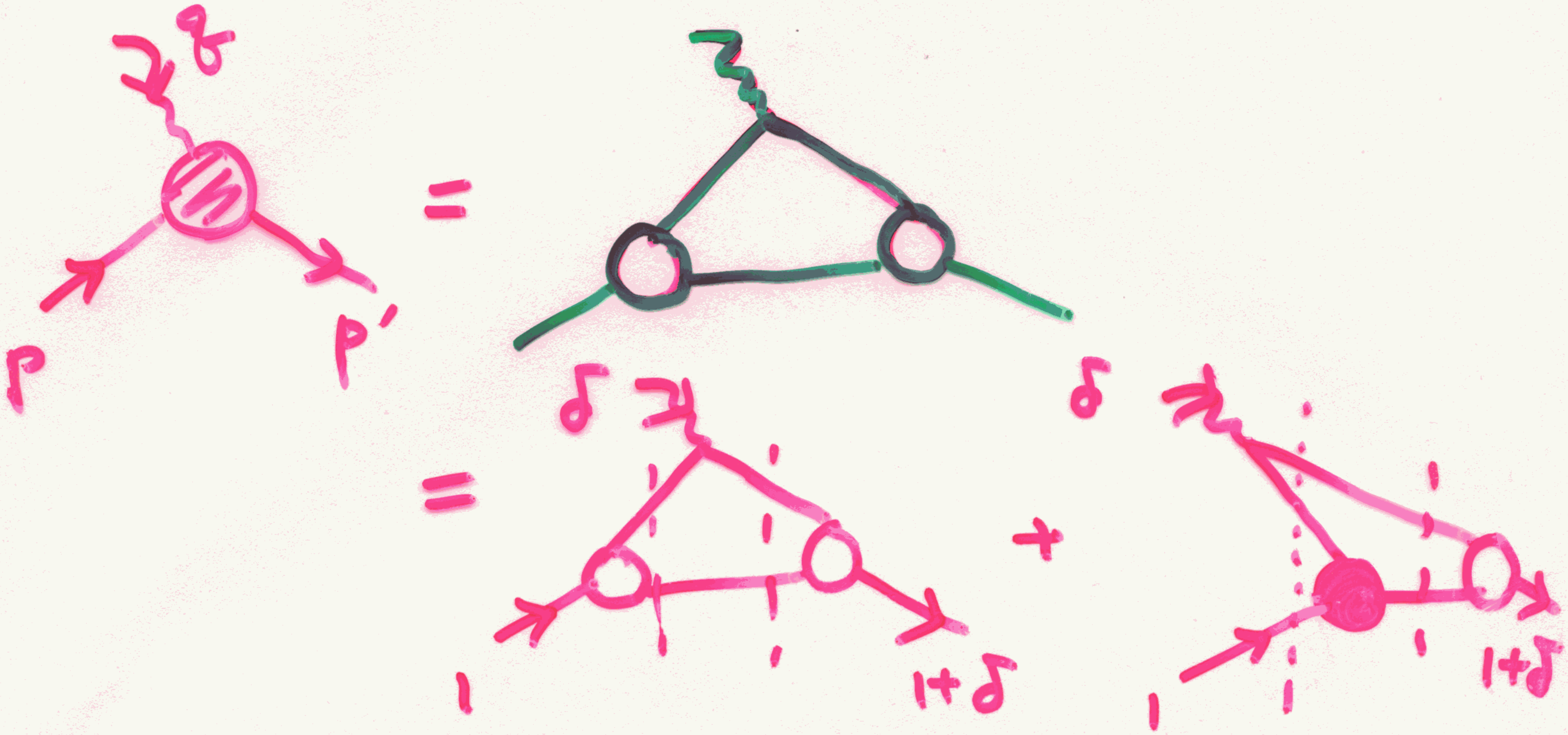

$$G_{00}^{+\,z.m.} = \lim_{\delta \to 0} \int_0^{\delta} \left(\cdots\cdots \right) dx$$

$$= \frac{1}{2p^{+}(2\pi)^3} \int d^2\vec{k}_\perp \frac{\ln\left[\dfrac{(\vec{k}_\perp - \vec{p}\,'_\perp)^2 + \Lambda^2}{(\vec{k}_\perp - \vec{p}_\perp)^2 + \Lambda^2}\right]}{\left[(\vec{k}_\perp - \vec{p}_\perp)^2 + \Lambda^2\right] - \left[(\vec{k}_\perp - \vec{p}\,'_\perp)^2 + \Lambda^2\right]}$$

$$\neq 0$$

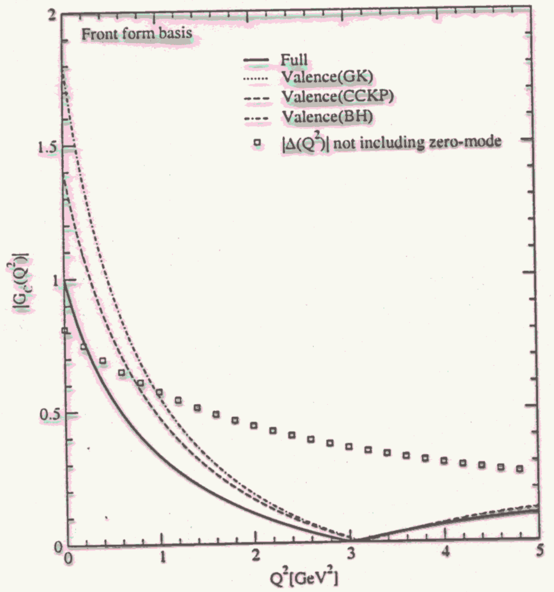

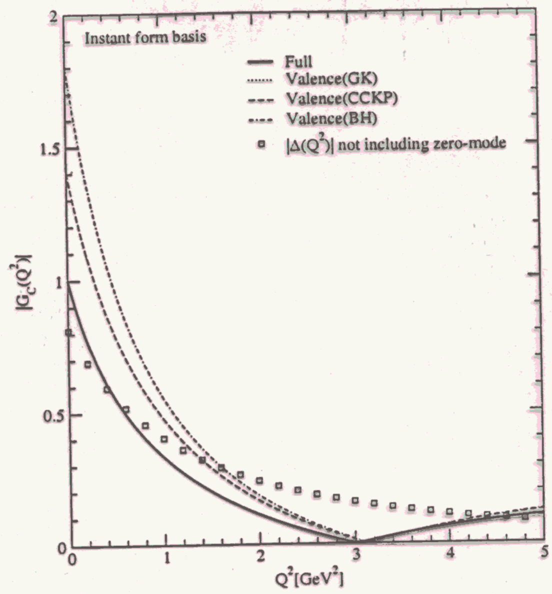

$m = 0.77\,GeV$

$m_g = 0.43\,GeV$

$\Lambda = 1.8\,GeV$

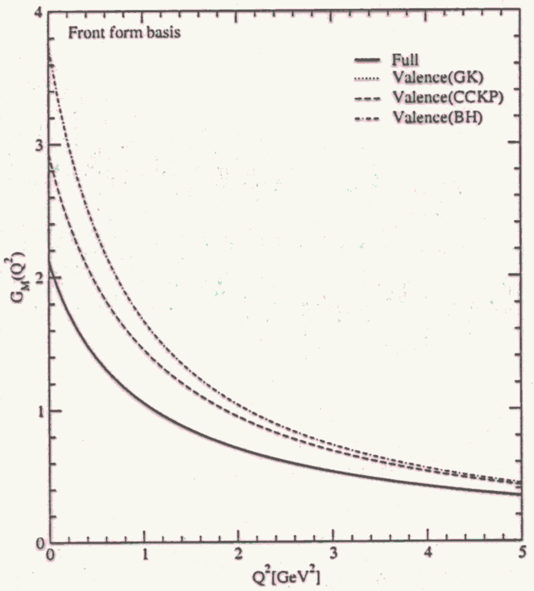

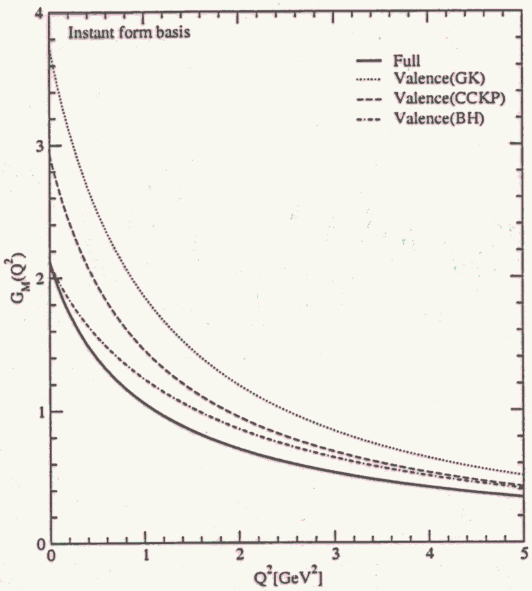

$f_\rho = 133.7\,MeV$

$f_{\rho^0}^{expt} = 152.8 \pm 3.6\,MeV$

$f_{\rho^\pm}^{expt} = 147.3\,MeV$

$\langle r_c^2 \rangle = 7.63\,GeV^{-2}$

$\mu_1 = 2.1$

$\langle r_M^2 \rangle = 9.73\,GeV^{-2}$

$Q_1 = 0.91$

$\langle r_Q^2 \rangle = 12.6\,GeV^{-2}$

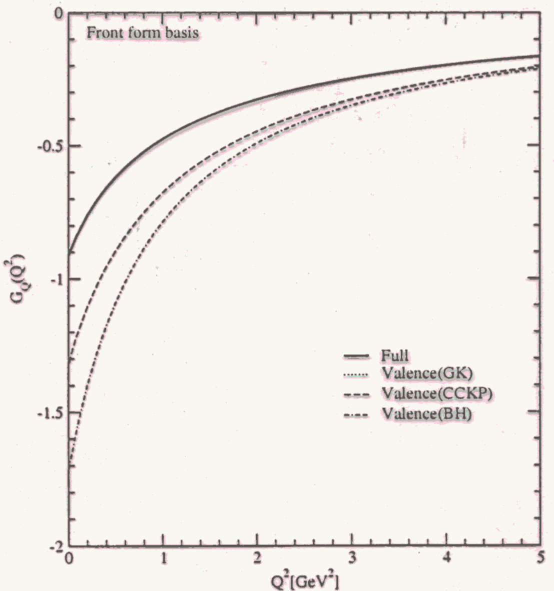

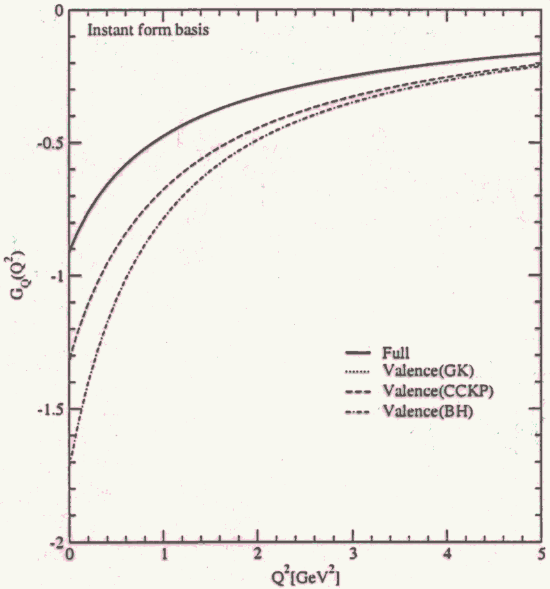

DYW

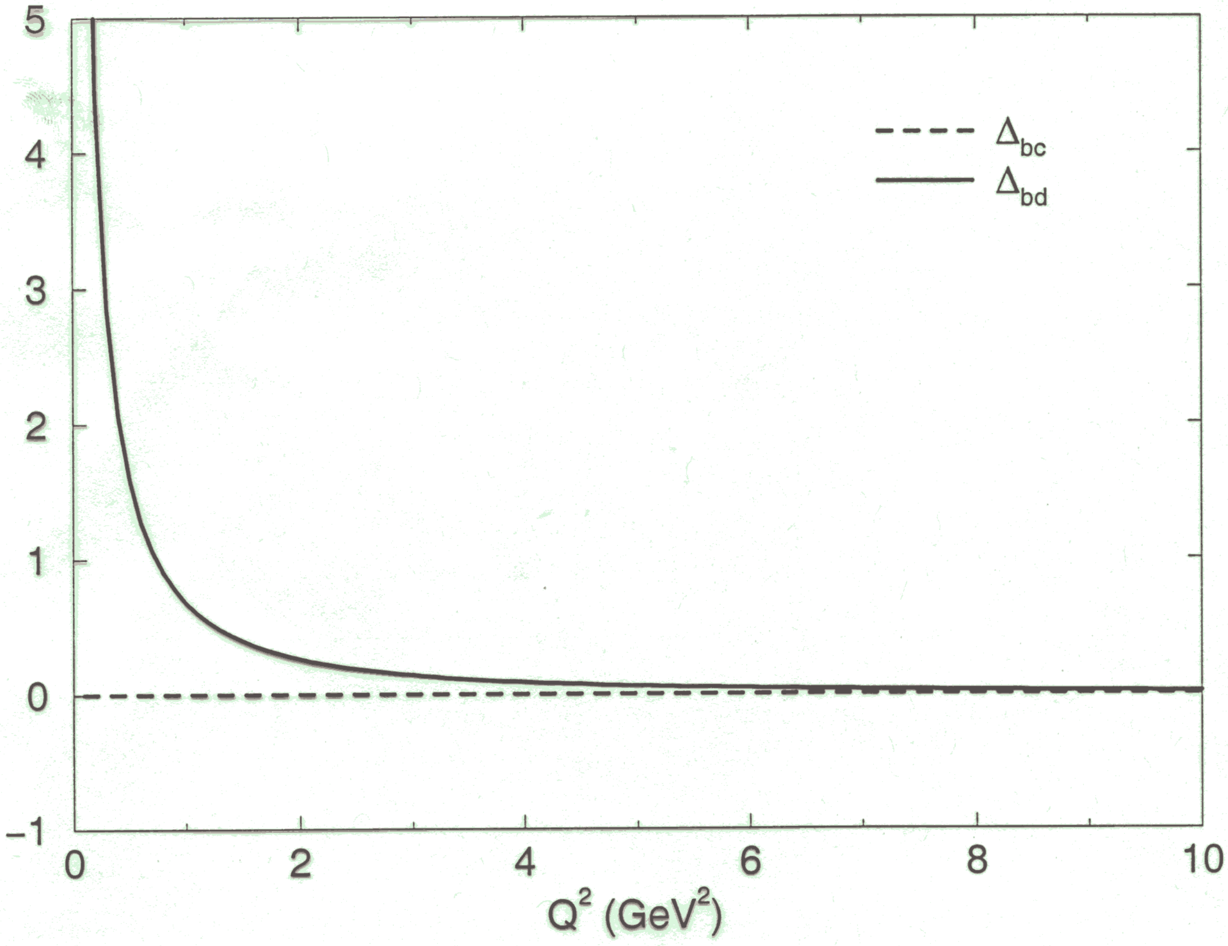

Common Belief of Equivalence

$$\begin{tikzcd}
& \text{Cov. Amp} \arrow[dl, "\int dk^0"'] \arrow[dr, "\int dk^-"] & \\
\text{Equal } t \arrow[rr, leftrightarrow, "\text{sum of diagrams}"'] & & \text{Equal } \tau
\end{tikzcd}$$

Fermion degrees of freedom in Equal τ is treacherous !

Bakker & Ji, PRD62, 074014 (00)

e.g. Triangle Fermion Loop in 1+1 Dim.

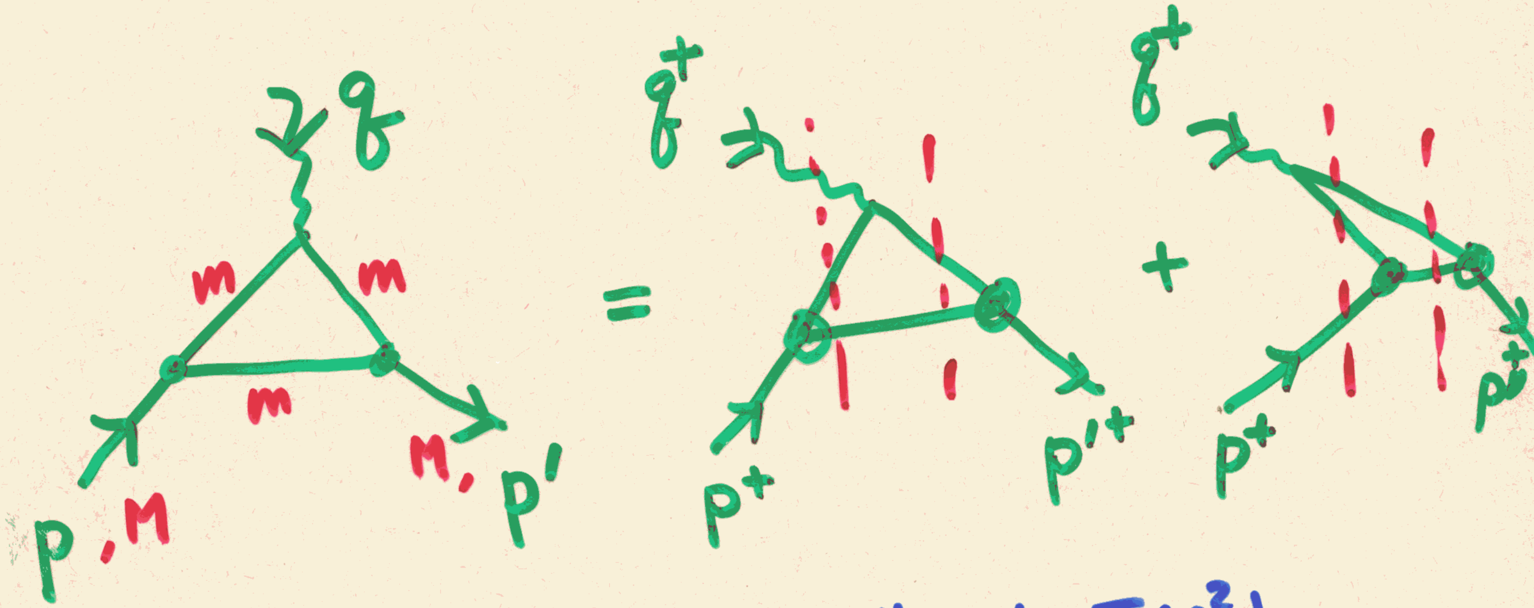

$$\langle p' | J^\mu | p \rangle = i e_M (p^\mu + p'^\mu) F(q^2)$$

$\mu = +$; $F\left(q^2 = -\frac{\alpha^2 M^2}{1+\alpha}\right)$

$$= \frac{N}{\pi(2+\alpha)} \left[\int_0^1 dx \frac{(1+\alpha)^2 m^2}{[m^2 - x(1-x)M^2][(1+\alpha)^2 m^2 - (1-x)(\alpha+x)M^2]} \right.$$

$$\left. + \int_0^\alpha dx \frac{(1+\alpha)(\alpha-x)[x(\alpha-x)M^2 - (1+\alpha)^2 m^2]}{\alpha[(\alpha-x)(1+x)M^2 - (1+\alpha)^2 m^2][x(\alpha-x)M^2 + (1+\alpha)m^2]} \right]$$

$\alpha \to 0$, 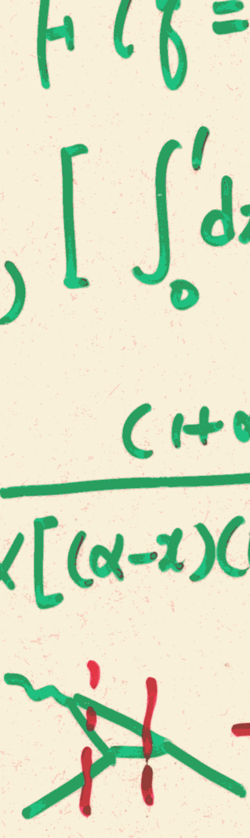 $\to 0$ (No zero mode!)

$\mu = -$, however ; $F\left(q^2 = -\frac{\alpha^2 M^2}{1+\alpha}\right)$

$$= \frac{N}{\pi(2+\alpha)}\left[\int_0^1 dx \frac{(1+\alpha)(1-x)^2 M^2}{[m^2 - x(1-x)M^2][(1+\alpha)^2 m^2 - (1-x)(\alpha+x)M^2]}\right.$$

$$\left. + \int_0^\alpha dx \frac{R(x,\alpha)}{\alpha - x}\right],$$

where

$$R(x,\alpha) = -\frac{(1+\alpha)^2 m^2\left[(1+\alpha)^2 m^2 + \{(1+\alpha)^2 - (1+x)\}(\alpha-x)M^2\right]}{\alpha M^2\left[(\alpha-x)(1+x)M^2 - (1+\alpha)^2 m^2\right]\left[x(\alpha-x)M^2 + (1+\alpha)m^2\right]}.$$

$\int_0^\alpha dx \frac{R(x,\alpha)}{\alpha - x}$ has an end-point singularity!

To get the same $F(q^2)$ as in $\mu = +$,

$R(\alpha,\alpha) = \frac{1+\alpha}{\alpha M^2}$ must be subtracted!

Even after subtracted,

$\int^\alpha \frac{R(x,\alpha) - R(\alpha,\alpha)}{\ldots} dx \not\to 0$ as $\alpha \to 0$ (Zero Mode

Fermion Loop in 3+1 Dim.

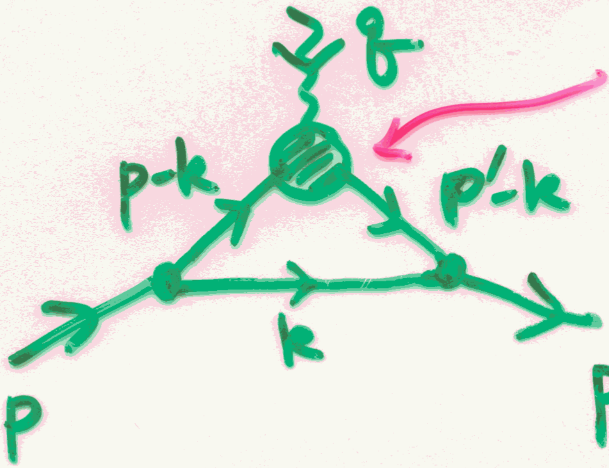

$\Gamma^\mu = S_\Lambda(p'-k)\,\gamma^\mu\, S_\Lambda(p-k)$

Pauli-Villars regularization

For finite Λ, neither UV divergence nor end-point singularity exist.

Even in the point vertex limit, i.e.

$\Gamma_\mu \to \gamma_\mu$ as $\Lambda \to \infty$,

the end-point singularity is removed completely although the result is logarithmically divergent as it must be in 3+1 dim.

Bakker, Choi, Ji, PRD 63, 074014 (01).

QCD CQM

Equal t	Equal $\tau = t + z/c$
$k^0 = \sqrt{\vec{k}^2 + m^2}$	$k^- = \dfrac{\vec{k}_\perp^2 + m^2}{k^+}$
Complicate Vac. → Simple Vac.	Simple Vac. → Simple Vac.
BCS (BV) Transf.	Zero-mode Cutoff
Coherent Vac. & Mass Gap Eq	Counter Terms & Mass Gap Eq.

Phenomenological LFCQM .

TABLES

TABLE I. The ground state meson masses. The $\omega-\phi$ and $\eta-\eta'$ mixing angles are predicted as $|\delta_V| = 4.2°$ and $\theta_{SU(3)} = \delta_P + 35.25° = -19°$, respectively.

$J^P = 0^-$	Experiment[MeV]	Theory	$J^P = 1^-$	Experiment	Theory
π	135±0.00035	135	ρ	770± 0.8	770
K	494± 0.016	470	K^*	892± 0.24	875
η	547± 0.19	547	ω	782± 0.12	782
η'	958±0.14	958	ϕ	1020±0.008	1020
D	1869±0.5	1821	D^*	2010± 0.5	2024
D_s	1969±0.6	2005	$M^a_{c\bar{s}}$ (D_s^*)	2112±0.7	2150
η_c	2980± 2.1	3128	J/ψ	3097±0.04	3257
B	5279± 1.8	5235	B^*	5325± 1.8	5349
B_s	5369±2.0	5378	$M_{b\bar{s}}$	–	5471
$M_{b\bar{b}}$	–	9295	Υ	9460± 0.21	9558

H.-M. Choi & C. Ji, PL B460, 461 (99)

PRD59, 074015 (99)

Variation principle implemented LFQM and application to ground state 0^- and 1^- nonets.

D. Arndt & C. Ji, PRD60, 094020 (99).

Radially excited mesons.

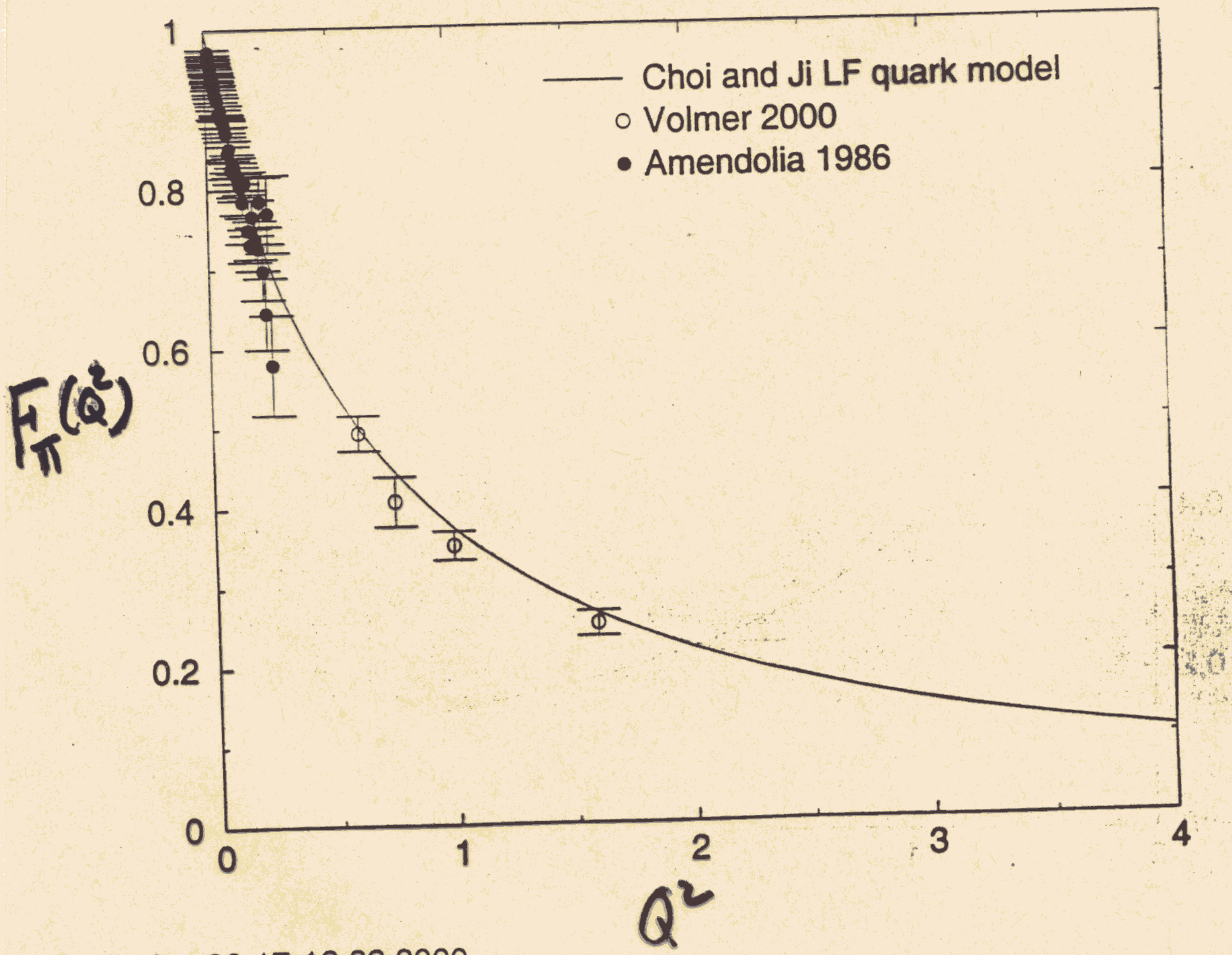

Mon Oct 30 17:13:32 2000

Timelike Processes

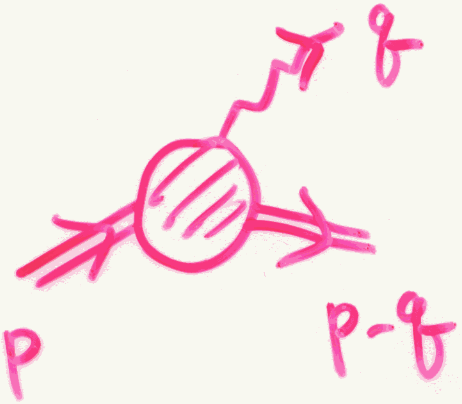

$$\boxed{q^2>0} = \sum_n$$

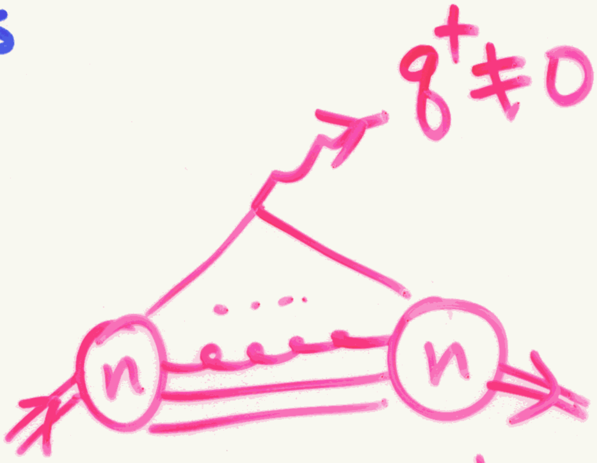

$q^2 = q^+q^- - \vec{q}_\perp^{\,2}$

$+ \sum_n$

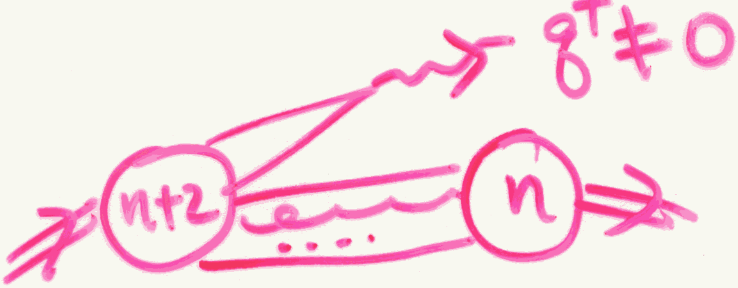

Brodsky & Hwang, NPB <u>543</u>, 239 (98).

CQM $\approx$

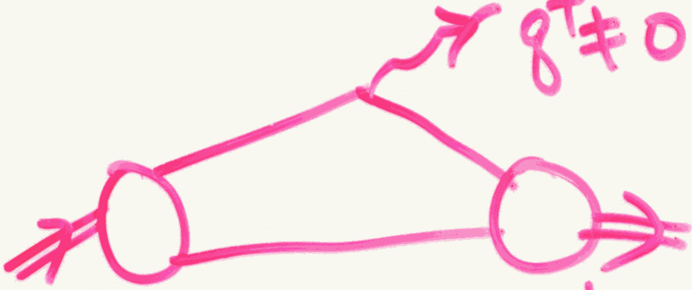

Embedded states +

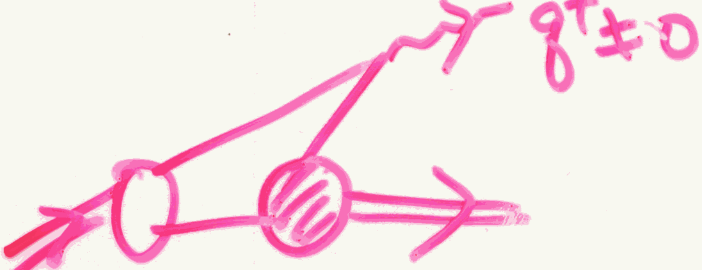

Bakker & Ji, PRD <u>62</u>, 074014 (00)

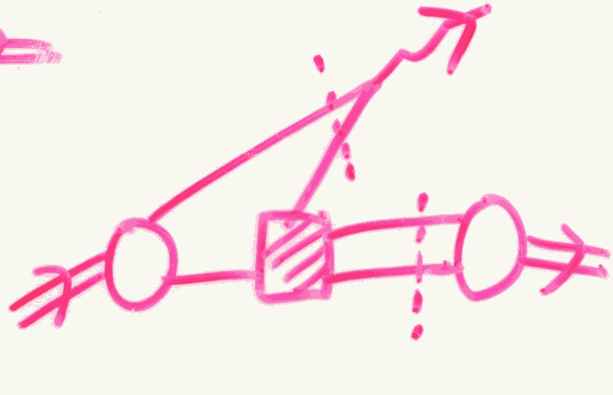

Effective treatment of embedded states

Ji & Choi, PL <u>B513</u>, 330 (01)

GPD Application : DVCS

$$\mathcal{M}_\pi^{\mu\nu}\left(\vec{q}_\perp, \vec{\Delta}_\perp, \zeta = \frac{\Delta^+}{p^+}\right) = i\int d^4z\, e^{-iq\cdot z}\langle p'|T\{J^\mu(z)J^\nu(0)\}|p\rangle$$

$$\epsilon_\mu(+)\,\epsilon^*_\nu(+)\,\mathcal{M}_\pi^{\mu\nu}(\vec{q}_\perp,\vec{\Delta}_\perp,\zeta) = -e_q^2\int_0^1 dx\left(\frac{1}{x-i\epsilon}+\frac{1}{x-\zeta+i\epsilon}\right)\mathcal{F}_\pi(x,\zeta,t)$$

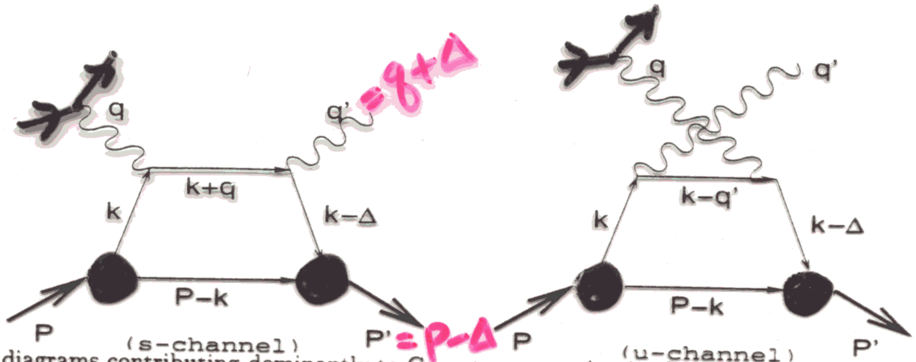

$t = \Delta^2$

FIG. 1. Handbag diagrams contributing dominantly to Compton scattering in the deeply virtual region. The lower soft part consists of a hadronic matrix element which is parametrized in the form of generalized parton distribution functions.

$$\mathcal{J}_\pi^+ \equiv \int \frac{dz^-}{4\pi}\, e^{ixp^+z^-/2}\langle p'|\bar\psi(0)\gamma^+\psi(z)|p\rangle\Big|_{z^+=\vec{z}_\perp=0}$$

$$= \mathcal{F}_\pi(x,\zeta,t)\,(p+p')^+$$

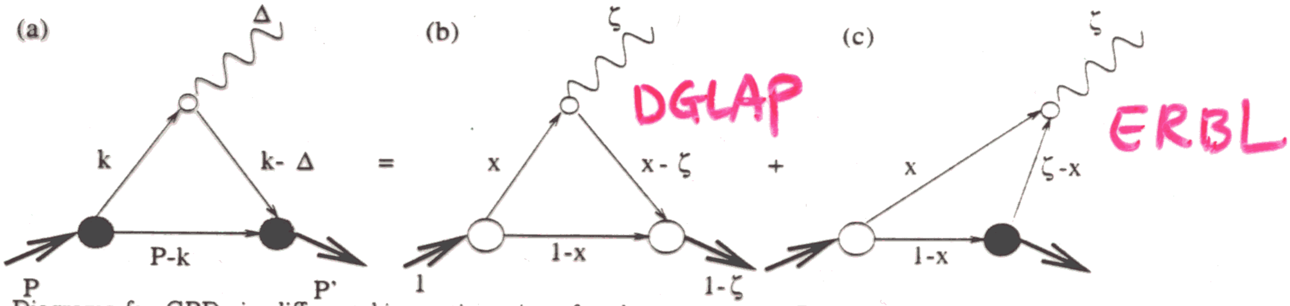

FIG. 2. Diagrams for GPDs in different kinematic regions for the case $\zeta > 0$: The covariant diagram (a) corresponds to the sum of the LF valence diagram (b) defined in DGLAP($\zeta < x < 1$) region and the nonvalence diagram (c) defined in ERBL($0 < x < \zeta$) region. The large white and black blobs at the meson-quark vertices in (b) and (c) represent the ordinary LF wave function and the nonvalence wave function vertices, respectively. The small white blob at the quark-gauge boson vertex indicates the nonlocality of the vertex.

$$J_\pi^+ \equiv \langle p'|\bar\psi(0)\gamma^+\psi(0)|p\rangle = F_\pi(t)\,(p+p')^+$$

Sum-Rules : $\displaystyle\int_0^1 \frac{dx}{1-\frac{\zeta}{2}}\,\mathcal{F}_\pi(x,\zeta,t) = F_\pi(t)$

$$\int_0^1 dx\, x^{n-1}\mathcal{F}_\pi(x,\zeta,t) = F_n(\zeta,t) \quad (n\geq 1)$$

Continuity at Crossover $x=\xi$

$$\mathcal{M}_{\gamma^*\pi\to\gamma\pi} \sim \int_0^1 dx\, \frac{F_\pi(x,\xi,t)}{x-\xi+i\epsilon}$$

$$= \underbrace{\mathcal{P}\int_0^1 dx\, \frac{F_\pi(x,\xi,t)}{x-\xi}}_{} + i\pi\, F_\pi(\xi,\xi,t)$$

$$\|$$

$$\lim_{\epsilon\to 0}\left[\int_0^{\xi-\epsilon} dx\, \frac{F_\pi(x,\xi,t)}{x-\xi} + \int_{\xi+\epsilon}^1 dx\, \frac{F_\pi(x,\xi,t)}{x-\xi}\right]$$

$$\int$$

$$\log\frac{1}{\epsilon}\cdot\left[F_\pi(\xi+\epsilon,\xi,t) - F_\pi(\xi-\epsilon,\xi,t)\right]$$

$$+ \text{ finite result}$$

- If $F_\pi(\xi_+) \neq F_\pi(\xi_-)$, then the real part blows up logarithmically as $\epsilon\to 0$.
- The imaginary part is given by the value of $F_\pi(\xi,\xi,t)$. $\longrightarrow$ SSA (Hermes, CLAS)

Test of Model Approximation

$$F_\pi(t) = \int_\xi^1 \frac{dx}{1-\frac{\xi}{2}} F_\pi^{val}(x,\xi,t) + \int_0^\xi \frac{dx}{1-\frac{\xi}{2}} F_\pi^{NV}(x,\xi,t)$$

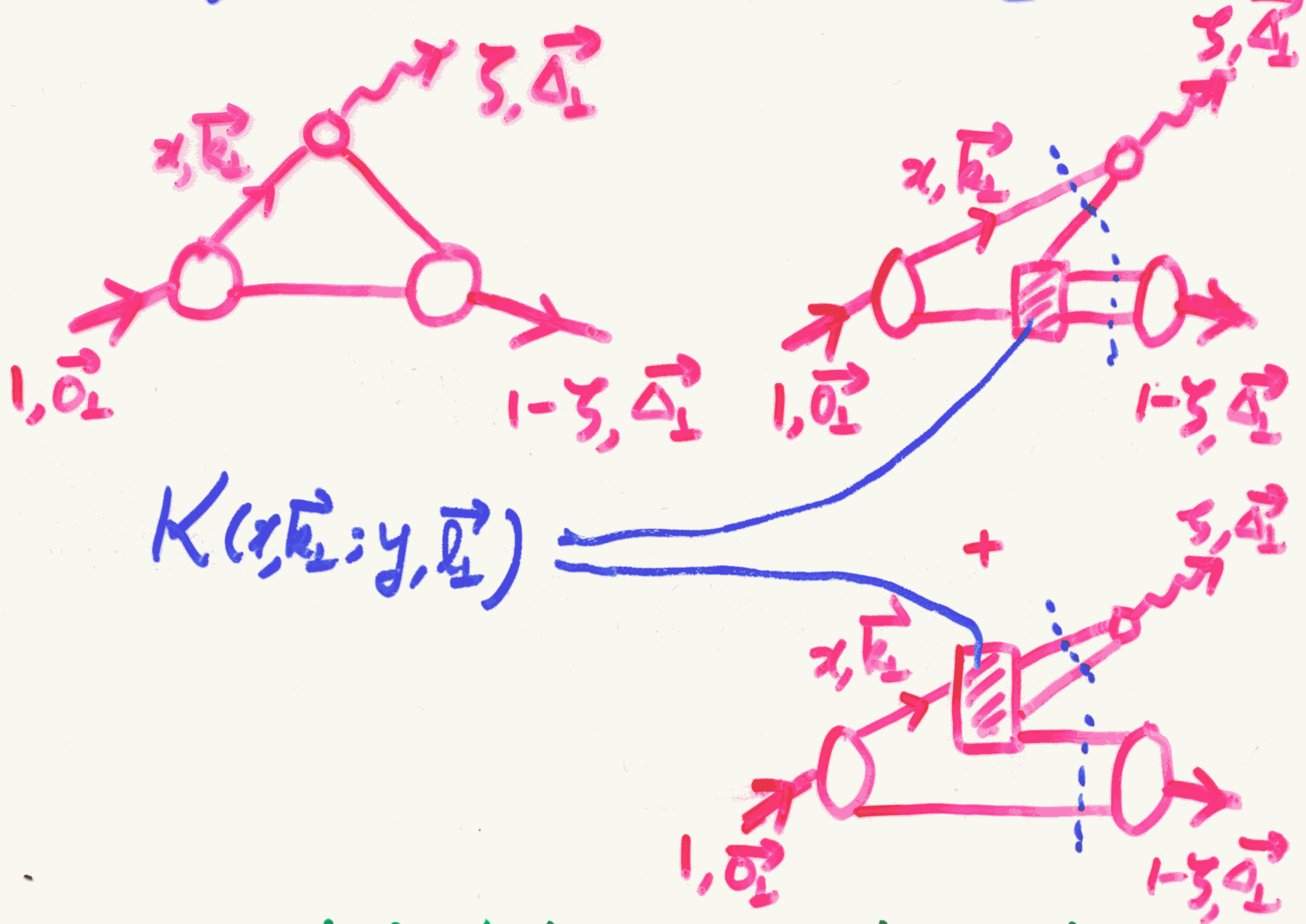

- Same kernel for both meson and gauge-boson wfs ensures the continuity of GPD and the cancellation of any infrared singularity that might occur in the kernel $K(x,\vec{k}_\perp;y,\vec{l}_\perp)$.

$$G_\pi \equiv \int_0^1 \frac{dy'}{y'(1-y')} \int d^2\vec{l}_\perp' \, \tilde{K}(x',\vec{k}_\perp'; y', \vec{l}_\perp') \, \chi_{(2\to 2)}(y', \vec{l}_\perp')$$

$$y' = \frac{y-\zeta}{1-\zeta}, \quad \vec{l}_\perp' = \vec{l}_\perp + y'\vec{\Delta}_\perp, \quad \tilde{K} = K\left[1 - \frac{S^+_{NV}(y,\vec{l}_\perp)\chi(y,\vec{l}_\perp)}{S^+_{NV}(x,\vec{k}_\perp)\chi(x,\vec{k}_\perp)}\right]$$

Fluctuations in G_π are neither unexpected nor troublesome.

- Nonval. contribution is highly suppressed in very small ζ region and large $-t$ region.

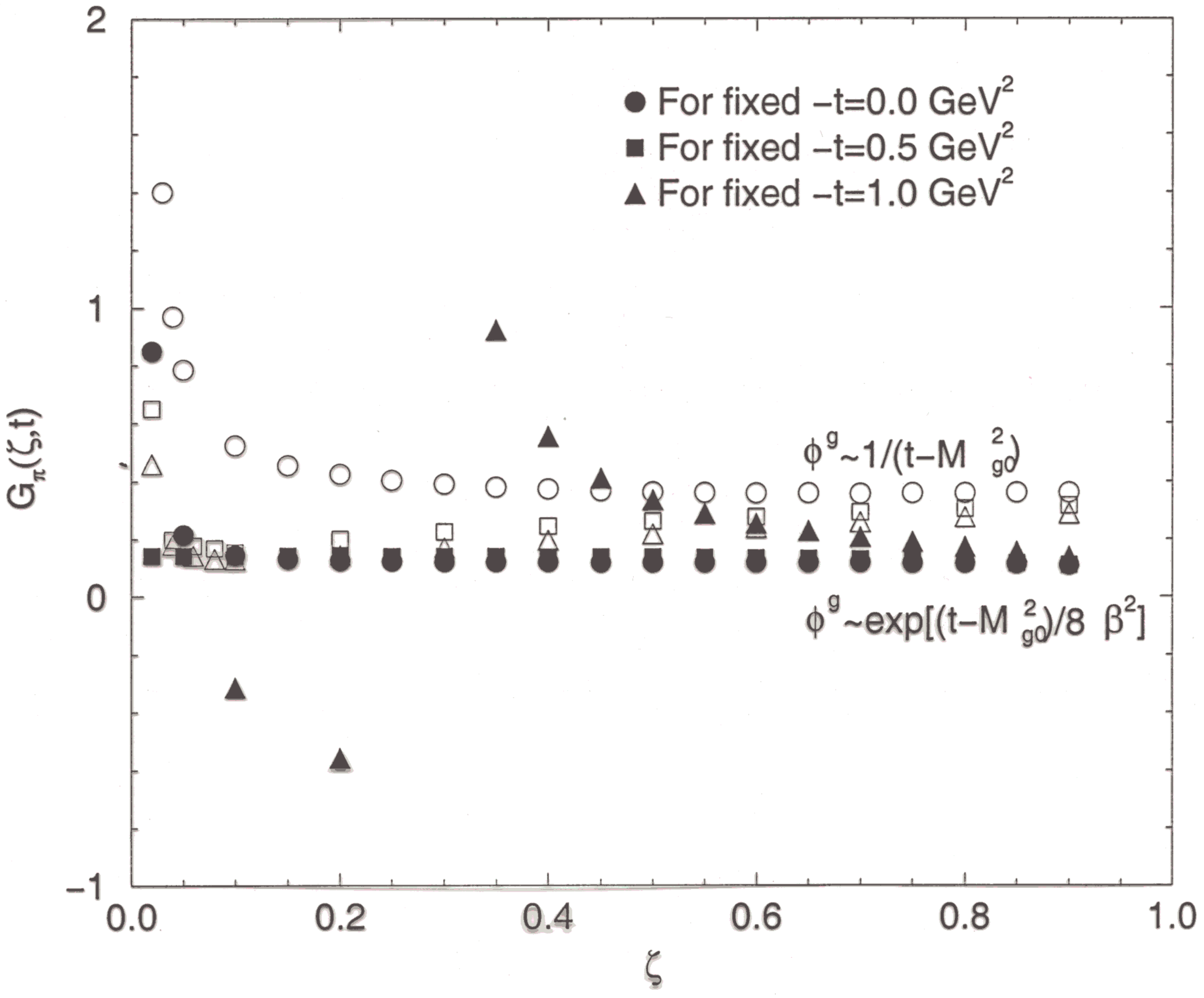

Choi, Ji, Kisslinger, PRD to appear

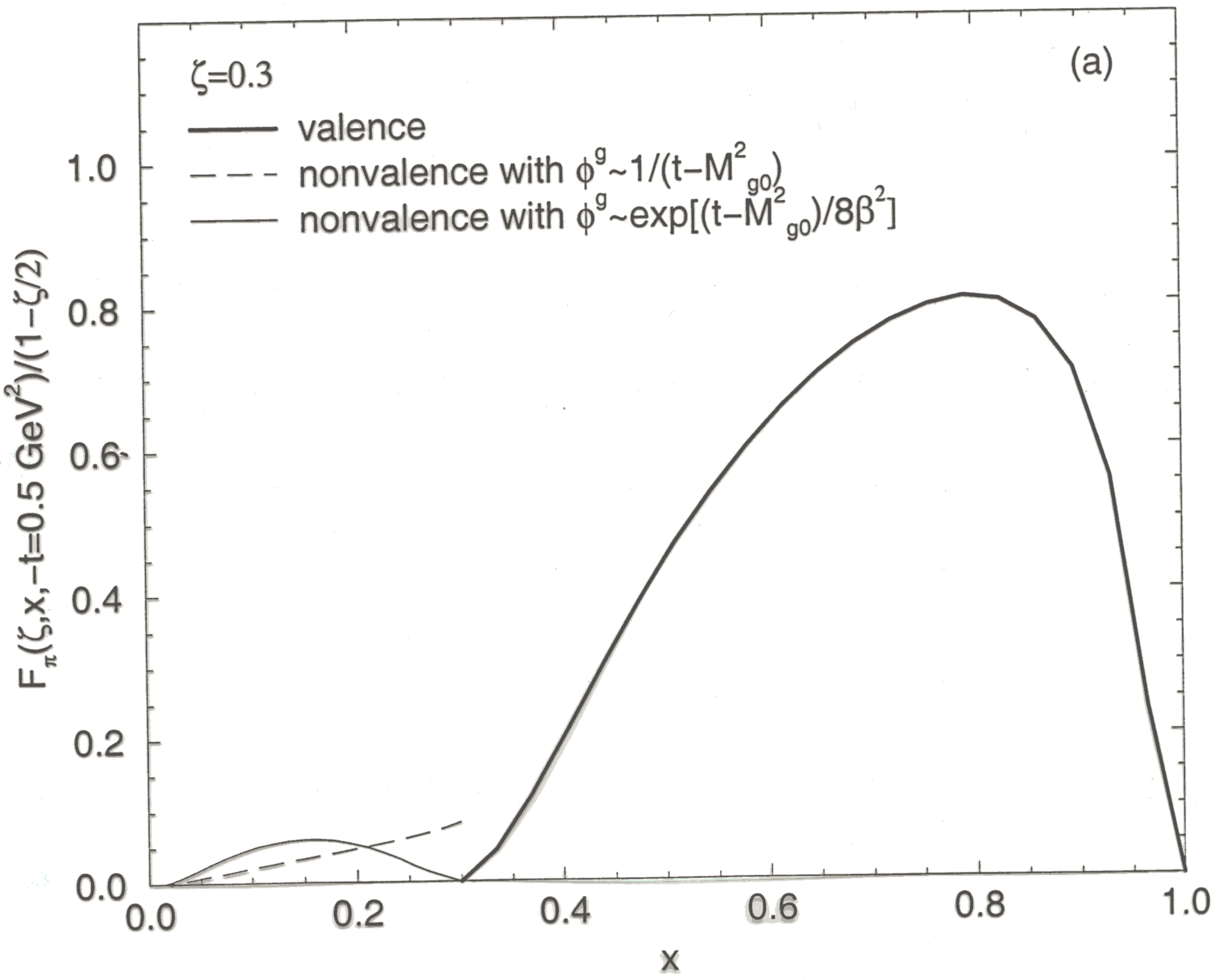

$\mathcal{F}_\pi(\zeta,\zeta,t) = 0$ Two-body

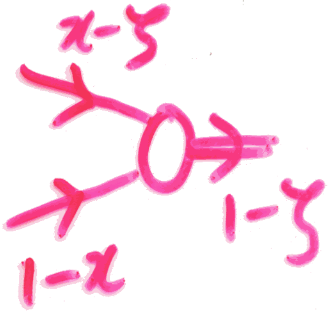

$\mathcal{F}_p(\zeta,\zeta,t) \neq 0$ Three-body

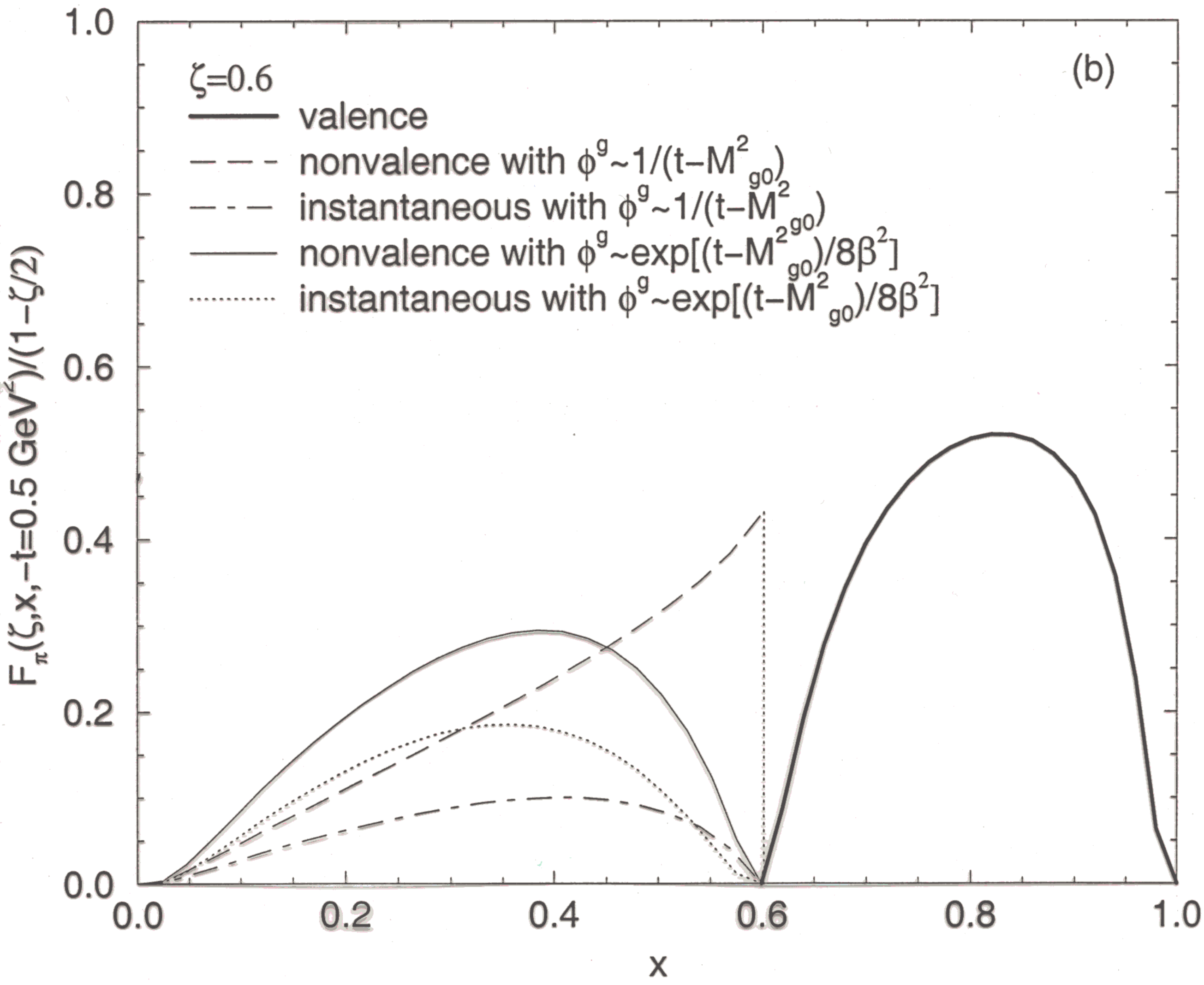

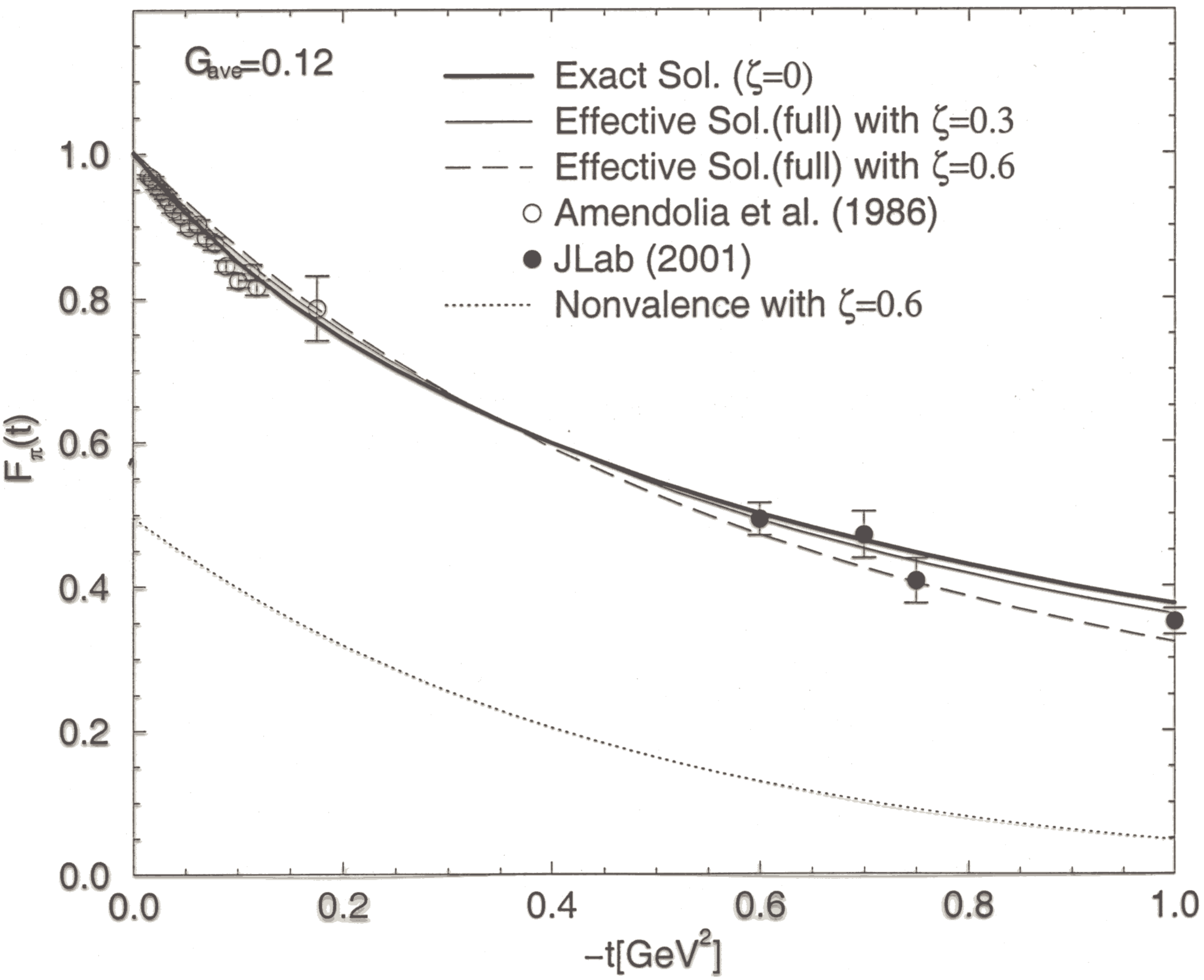

G_{ave}=0.12
Exact Sol. (ζ=0)
Effective Sol.(full) with ζ=0.3
Effective Sol.(full) with ζ=0.6
Amendolia et al. (1986)
JLab (2001)
Nonvalence with ζ=0.6
$F_\pi(t)$
$-t[\mathrm{GeV}^2]$
0.0
0.2
0.4
0.6
0.8
1.0

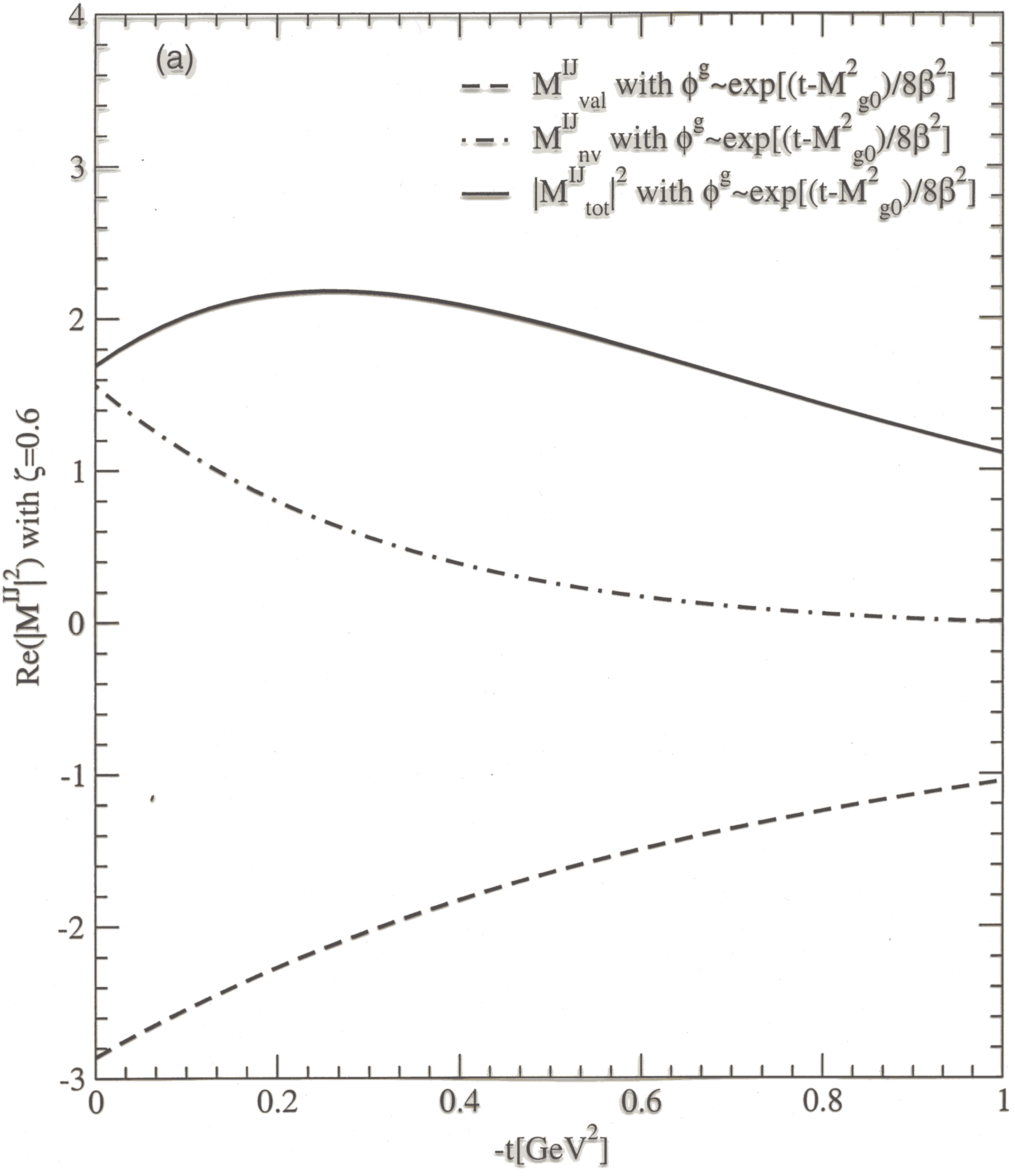
(a)
M^{IJ}_{val} with ϕ^g~exp[(t-M^2_{g0})/8β^2]
M^{IJ}_{nv} with ϕ^g~exp[(t-M^2_{g0})/8β^2]
$|M^{IJ}_{tot}|^2$ with ϕ^g~exp[(t-M^2_{g0})/8β^2]
Re($|M^{IJ}|^2$) with ζ=0.6
-t[GeV^2]
4
3
2
1
0
-1
-2
-3
0
0.2
0.4
0.6
0.8
1

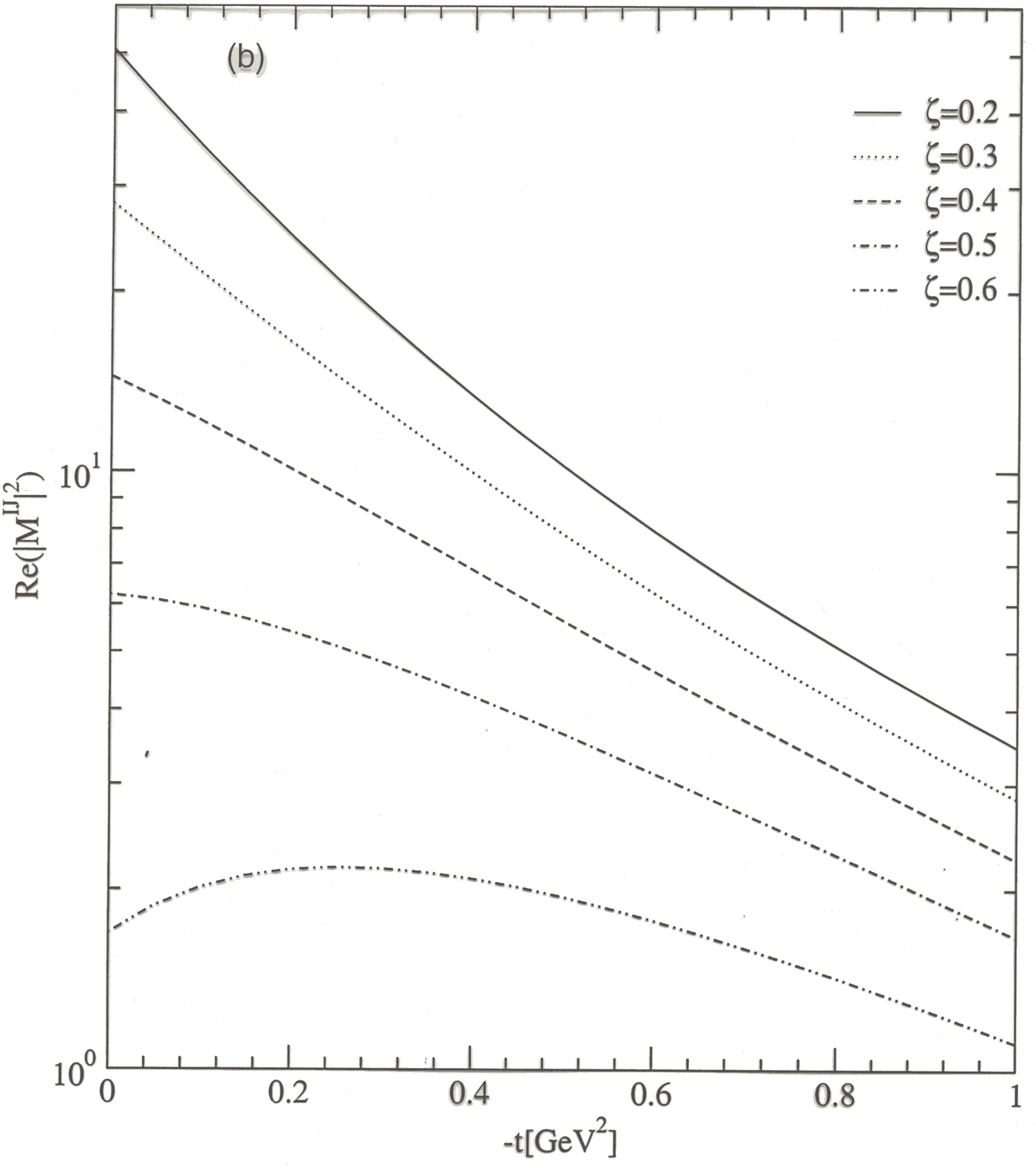
(b)
ζ=0.2
ζ=0.3
ζ=0.4
ζ=0.5
ζ=0.6
10^1
10^0
0
0.2
0.4
0.6
0.8
1
$Re(|M^{IJ}|^2)$
$-t[GeV^2]$

$$F_2^{I=0}(\xi, t=0) = \frac{1}{2}(1 + C\xi^2)$$

$C = -\frac{1}{4}$ (chiral limit)

-0.2843 (LFCQM)

Polyakov & Weiss, PRD 60, 114017 (99).

D-term

in Chiral-quark-soliton model.

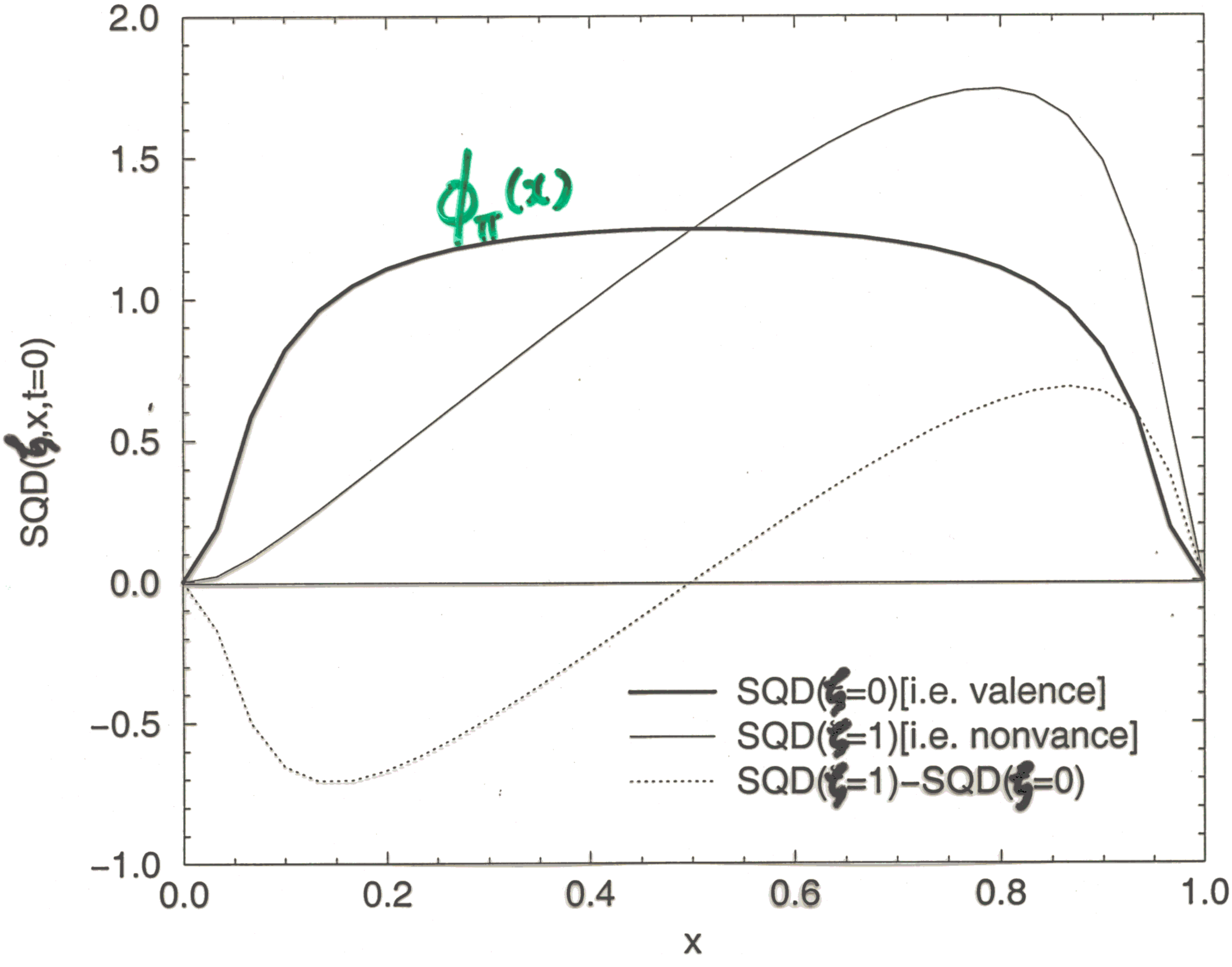

Conclusions and Discussions

1. Although caveats exist,
   LFD approach provides in general an effective and useful tool to analyze the processes involving hadrons for entire mom. transf. region.

2. Utilizing distinguished features of vacuum and rotation on the LF, the more reliable CQM can be constructed for hadron phenomenology.

3. LFCQM is now applied to GPD and useful informations are obtained especially from $\mathcal{F}_\pi(x \approx \zeta, \zeta, t)$.
   Continuity at $x = \zeta$; $\mathcal{F}_p(\zeta, \zeta, t) \neq 0$
   higher Fock-states ~ T-odd, SSA.

4. Challenges remain to understand the caveats more clearly so that we may control them in phenomenology and need to extend the model to three-body bound-states and beyond.